Journal of Solid State Chemistry 184 (2011) 236–240

Contents lists available at ScienceDirect

Journal of Solid State Chemistry

journal homepage: www.elsevier.com/locate/jssc

Distribution-related luminescence of Eu^{3+} sensitized by SnO_2 nano-crystals embedding in oxide glassy matrix

Yunlong Yu, Daqin Chen, Ping Huang, Hang Lin, Anping Yang, Yuansheng Wang *

State Key Laboratory of Structural Chemistry, Fujian Institute of Research on the Structure of Matter, Chinese Academy of Sciences, Fuzhou, Fujian 350002, China

ARTICLE INFO

Article history:
Received 10 August 2010
Received in revised form
12 November 2010
Accepted 16 November 2010
Available online 20 November 2010

Keywords:
SnO_2 nano-crystals
Eu^{3+}
Energy transfer
Glass ceramics
Melt quenching

ABSTRACT

Eu^{3+} doped transparent glass ceramics embedding SnO_2 nano-crystals were prepared by melt quenching and subsequent heating. Site selective excitation experiments revealed that some Eu^{3+} ions were incorporated in the SnO_2 lattices by substituting Sn^{4+} ions, whereas the rest located in the oxide glassy matrix. Interestingly, it is found that the Eu^{3+} ions residing in the SnO_2 lattices exhibited much longer luminescent decay lifetime than those in the glassy matrix. Measurements on the photoluminescence excitation and photoluminescence spectra demonstrated the occurrence of energy transfer from the SnO_2 nano-crystals to the Eu^{3+} ions. The influences of Eu^{3+} content, and furthermore, their location on the energy transfer process were discussed.

1. Introduction

Rare earth (RE) ions doped semiconductor nano-crystals have attracted a great deal of interest because of their unique optical properties and potential applications in many fields such as fluorescent lamps, optical communications and flat-panel displays [1–3]. In these nano-materials, the semiconductor hosts with large absorption cross-section can act as sensitizers to promote RE emissions by harvesting the excitation photon energy and then transferring it to the RE ions. Another advantage is that the optical properties could be tailored via size and shape control of the semiconductor, which is very attractive in fabricating nano-devices [4,5]. However, handling of the nano-particles is quite difficult because of their continuous growth and agglomeration during storage [6,7]. One of the ways to circumvent this problem is to disperse nano-sized semiconductors in transparent glassy matrix. Such nano-structured composite may possess not only unique optical properties from the semiconductor, but also excellent chemical and mechanical performances from the glassy matrix [8]. Owing to the much smaller size of the nano-particles than the wavelength of the visible light, or the matching of the refractive indexes between the semiconductor and the glassy matrix, the nano-composite exhibits a high transparency.

The RE doped SiO_2 amorphous matrices containing Si nano-crystals, prepared by co-sputtering or ion-implantation, have been reported in recent years. The relevant studies evidenced the energy transfer from the Si nano-crystals to the RE ions [9–11]. However, thermal quenching, a fatal drawback for optical applications, emerged in these materials because of the small indirect band gap of the Si semiconductor [12–14]. More recently, in order to eliminate the energy back transfer effect, the RE doped silica containing semiconductor nano-crystals with large band gaps, such as ZnO, SnO_2 and In_2O_3, prepared by the sol–gel method have been reported [15–17]. Owing to the efficient energy transfer from the semiconductor nano-particles to the RE ions, the RE emission were greatly intensified. Unfortunately, such materials usually exhibit a relatively short emission lifetime and low quantum efficiency due to the large amount of residual hydroxyl quenching groups in the sol–gel system [1,18–20]. In addition, the mechanical performance of the sol–gel monolithic material is not suitable for practical applications.

To fabricate the SiO_2-based bulk composite containing semiconductor nano-crystals, the route based on melt quenching, which is commonly used to fabricate the traditional inorganic glasses, might be a desirable alternative. However, to our knowledge, few investigations on the energy transfer between RE ions and semiconductor nano-crystals embedded in oxide glassy matrix prepared by melt quenching were reported so far [14,21]. Especially, the incorporation of RE ions into the nano-crystals has not been confirmed. As a result, it is difficult to investigate the relation between the energy transfer and the distribution of the RE ions. On the other hand, SnO_2 is a well know wide band gap (E_g=3.6 eV) n-type semiconductor with potential applications in gas sensors, dye-based solar cells and catalyst supports [22–24]. Works about optical properties of different RE ions doped SnO_2 nano-crystals have appeared recently; the studies demonstrated that the luminescent ions can be partially

* Corresponding author. Fax: +86 591 8370 5402.
E-mail address: yswang@fjirsm.ac.cn (Y. Wang).

0022-4596/$ - see front matter © 2010 Elsevier Inc. All rights reserved.
doi:10.1016/j.jssc.2010.11.021

introduced in the nano-crystals [25–27]. Therefore, in this paper, the Eu^{3+} doped glass ceramics embedding SnO_2 nano-crystals were successfully prepared by melt quenching and subsequent heating. The distribution of Eu^{3+} ions, the energy transfer process between SnO_2 and Eu^{3+}, and the related luminescence were systematically investigated.

2. Experimental details

The compositions of the materials were as follows (in mol%): $17Na_2O–10CaO–6Al_2O_3–64SiO_2–3SnO_2$ (for comparison, some samples without SnO_2 were also prepared). The doped Eu^{3+} ions, with content of 0.1, 0.5, 1.0 and 2.0 mol%, respectively, were introduced by addition of Eu_2O_3 in appropriate amount. The mixed chemicals were melted in a covered Pt crucible at 1500 °C for 1 h in the ambient atmosphere, then poured into a 300 °C preheated copper mold, and cooled down to room temperature to form the precursor glass. The precursor glass was cut into 1 cm^2 coupons and heat treated at 600 °C for 2 h to form glass ceramic through crystallization.

The actual elemental contents of the as-prepared glass were measured by Inductively Coupled Plasma OES spectrometer (ICP, Ultima2). The contents of Na, Ca, Al, Sn and Eu were directly measured, while the contents of Si and O could be derived from the experimental data. To identify the crystalline phase, X-ray diffraction (XRD) analysis was carried out with a powder diffractometer (DMAX2500) using Cu$K\alpha$ radiation (λ=0.154 nm). The microstructures of the samples were studied using a transmission electron microscope (TEM, JEM-2010) operated at 200 kV. TEM specimens were prepared by dispersing the fine power grinded from the bulk sample in ethanol, followed by ultrasonic agitation, and then depositing onto a carbon enhanced copper grid. The photoluminescence excitation (PLE) and photoluminescence (PL) spectra, under the excitation of a xenon lamp (450 W) equipped with a grating monochromator, were recorded by a PMT detector (R928). For the spectroscopic measurements, the finely surface-polished samples with the same geometry of $1 \times 1 \times 0.5$ cm^3 were placed perpendicular to the excitation light.

3. Results and discussion

The ICP measured elemental contents of the $17Na_2O–10CaO–6Al_2O_3–64SiO_2–3SnO_2–1Eu_2O_3$ glass, together with the nominal ones, are shown in Table 1. Evidently, the measured composition is basically consistent with the nominal one. The reductions of the measured Na and Ca contents are due to thermal evaporation of Na_2O and CaO with relatively lower melting points during heating. XRD spectrum of the Eu^{3+}-free glass ceramic, shown in Fig. 1, presents a diffuse hump originated from the glassy matrix and several diffraction peaks assigned to the tetragonal rutile SnO_2 (PDF 71-0652). The mean size of the nano-crystals was evaluated to be about 9 nm by the Scherrer equation. TEM micrograph and the corresponding selected area electron diffraction (SAED) pattern of the glass ceramic heat treated at 600 °C for 2 h, as shown in Fig. 2a, shows that SnO_2 particles with sizes of 5–12 nm disperse homogeneously in the glassy matrix. High-resolution TEM (HRTEM) image shown in Fig. 2b reveals the detailed lattice structure of an individual SnO_2 nano-crystal. The corresponding fast Fourier transform (FFT) pattern, shown in Fig. 2c, exhibits the diffraction pattern of the tetragonal SnO_2 along the [00$\bar{1}$] zone axis.

Table 1
Nominal and measured elemental contents in $17Na_2O–10CaO–6Al_2O_3–64SiO_2–3SnO_2–1Eu_2O_3$ glass.

Element	Nominal (at%)	Measured (at%)
Na	11.07	8.82
Ca	3.26	2.89
Al	3.91	4.64
Sn	0.98	0.99
Eu	0.65	0.67
Si	20.85	21.58
O	59.28	60.41

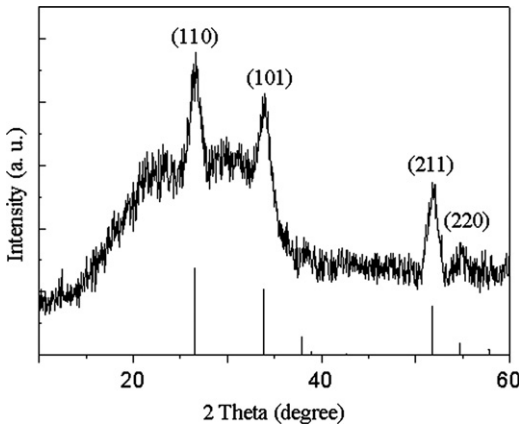

Fig. 1. XRD spectrum of Eu^{3+}-free glass ceramic. The standard spectrum of rutile SnO_2 (PDF 71-0652) is shown at the bottom.

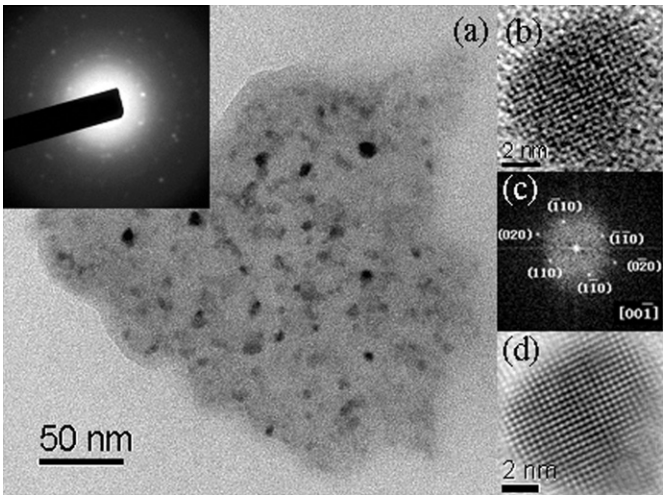

Fig. 2. (a) TEM micrograph and the corresponding SAED pattern of Eu^{3+}-free glass ceramic; (b) HRTEM image of an individual SnO_2 nano-crystal and (c, d) FFT pattern and the filtered HRTEM image from the SnO_2 nano-crystal in (b).

The PLE and PL spectra of the Eu^{3+}-free glass ceramic are shown in Fig. 3a. On the PLE spectrum monitored at the wavelength of 465 nm, a broad excitation band with a maximum at 335 nm (3.71 eV) is observed, which reveals a wider bang gap for SnO_2 nano-crystals than their bulk counterpart (3.6 eV) owing to the quantum confinement. The PL spectrum, under 335 nm excitation, shows a unique broad emission band ranged from 1.72 to 3.45 eV and centered at 465 nm. As a comparison, no emission band was detected under the same experimental conditions for the Eu^{3+}-free sample without SnO_2, indicating that the blue emission band is assigned to the SnO_2 nano-crystals. Such luminescence is generally regarded attributing to the radiative recombination of the photogenerated holes with the electrons occupying the oxygen vacancies in the semiconductor [28,29].

Fig. 3b shows the PLE spectra of the 0.5 mol% Eu^{3+} doped samples with and without SnO_2, respectively, by monitoring the 588 nm emission. The intensity is normalized to the strongest peak.

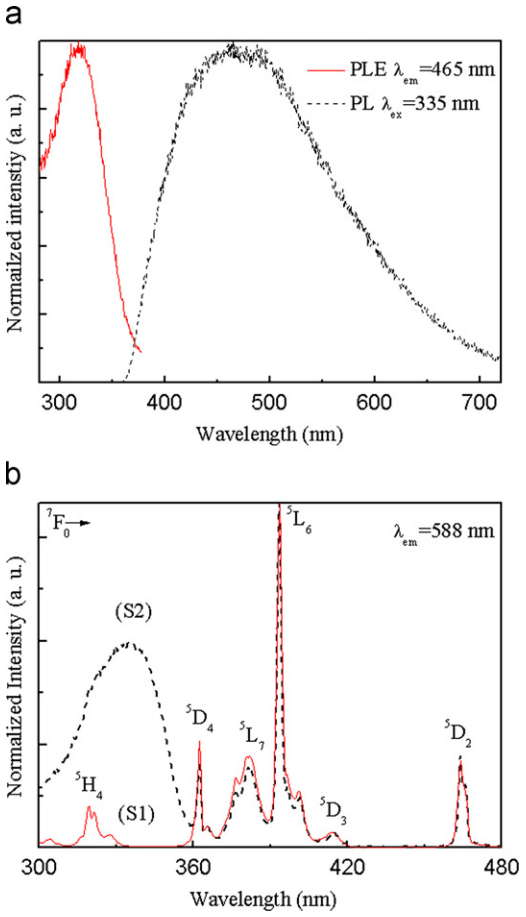

Fig. 3. (a) PLE and PL spectra of Eu^{3+}-free glass ceramic, (b) PLE spectra of 0.5 mol% Eu^{3+} doped samples by monitoring $^5D_0 \rightarrow {}^7F_1$ emission at 588 nm (S1: glass without SnO_2; S2: glass ceramic).

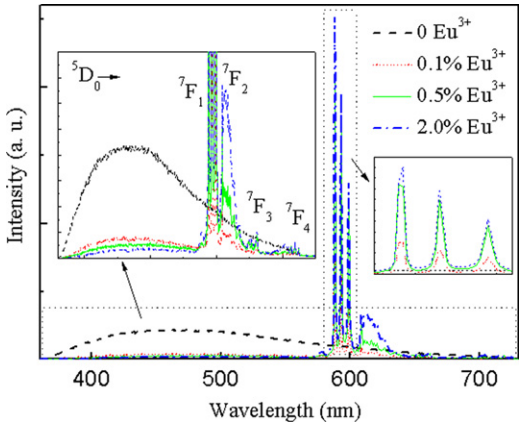

Fig. 4. PL spectra of glass ceramics doped with various contents of Eu^{3+}.

Both spectra exhibit several sharp Eu^{3+} intrinsic peaks, while an additional broad band with a maximum at 335 nm appears in the spectrum of the glass ceramic. The line-shape of this excitation band is similar to the one for the SnO_2 blue emission shown in Fig. 3a, suggesting that the emission of Eu^{3+} could be excited by the SnO_2 nano-crystals via an effective energy transfer.

Aiming to further explore the energy transfer between the SnO_2 nano-crystals and the Eu^{3+} ions, the emission spectra for the glass ceramics doped with various contents of Eu^{3+} were measured, as shown in Fig. 4. The excitation wavelength of 335 nm was adopted in order to permit merely the excitation of SnO_2 nano-crystals while avoiding the direct excitation of Eu^{3+}. The Eu^{3+}-free sample exhibits only one broad blue emission band. Upon Eu^{3+} addition, several sharp emission peaks corresponding to the Eu^{3+}:$^5D_0 \rightarrow {}^4F_J$ (J=0, 1, 2, 3 and 4, respectively) transitions are clearly observed. With increasing of Eu^{3+} content, the emission of Eu^{3+} intensifies while that of SnO_2 weakens monotonically. Based on these results, the energy transfer process is speculated as follows: the electron–hole pairs, generated by the band gap excitation of SnO_2, recombine and then transfer a part of the energy to the nearby Eu^{3+} ions to promote their electrons from the ground state to the excited ones, inducing the Eu^{3+} emission via a radiative relaxation. With increasing of Eu^{3+} content, the amount of energy transferred from SnO_2 to Eu^{3+} increases, resulting naturally in the intensification of Eu^{3+} emission and the quenching of SnO_2 emission.

Remarkably, under excitation at 335 nm, the Eu^{3+}: $^5D_0 \rightarrow {}^7F_1$ transition of the 0.5 mol% Eu^{3+} doped glass ceramic exhibits three well-resolved sharp and intense peaks located at 588, 593 and 599 nm, as shown in Fig. 5, strongly suggesting that, in spite of the biggish difference between the radius of Eu^{3+} (0.095 nm) and that of Sn^{4+} (0.076 nm), some of the Eu^{3+} ions are incorporated in the SnO_2 lattices by substituting Sn^{4+} ions at the C_{2h} or D_{2h} sites [26,27,30,31]. In fact, there are two possible channels for the Eu^{3+} excitation in the samples. One is the excitation of SnO_2 followed by an energy transfer from SnO_2 to Eu^{3+} (indirect excitation), and the other is the direct excitation of Eu^{3+} ions from the ground state to the excited ones, such as the case of 465 nm excitation. It is noticed that, under the excitation at 465 nm (in this case all the Eu^{3+} ions might be excited), the line-shape of PL spectrum of the glass ceramic is similar to that of the glass without SnO_2, and no well-resolved Stark components are found, as shown in Fig. 5, implying that only a small portion of Eu^{3+} is incorporated into SnO_2 nano-crystals, which is not surprising taking into account the low solubility of lanthanide ions in the bulk SnO_2 (around 0.05% [32]). The line-shape of the PL spectrum of the glass ceramic under the indirect excitation at 335 nm is quite different from that under the direct excitation at 465 nm, revealing that only a part of Eu^{3+} ions are sensitized by SnO_2. In spite of this, for the Eu^{3+}:$^5D_0 \rightarrow {}^7F_1$ emission the indirect excitation of SnO_2 is much efficient than the intrinsic $^7F_0 \rightarrow {}^5H_4$ excitation of Eu^{3+} (as shown in Fig. 3b). It is known that the intensity ratio of the electric dipole transition to the magnetic dipole one, i.e., $^5D_0 \rightarrow {}^7F_2/{}^5D_0 \rightarrow {}^7F_1$, is strongly related to the coordination structure of Eu^{3+} ions. Because of the selective excitation of Eu^{3+} ions located in the ordered SnO_2 lattices, the transition intensity ratio measured by the indirect excitation at 335 nm is much smaller than that obtained by the direct excitation at 465 nm.

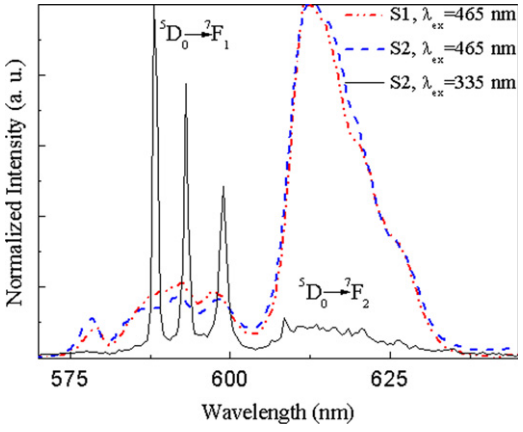

Fig. 5. PL spectra of 0.5 mol% Eu^{3+} doped samples excited at 465 and 335 nm, respectively. (S1: glass without SnO_2; S2: glass ceramic).

As is well known, the electric dipole transition $^5D_0 \rightarrow {}^7F_2$ should be totally forbidden if the Eu^{3+} ions are right at the Sn^{4+} site of the D_{2h} or C_{2h} point symmetry.[24,25] However, under the indirect excitation at 335 nm, a broad emission band centered at 614 nm with some weak peaks, ascribing to the $^5D_0 \rightarrow {}^7F_2$ transition, is observed, as shown in Fig. 5. The broad band might be attributed to the Eu^{3+} ions located at the disordered sites, i.e., in the glass matrix, while the weak peaks are possibly induced by the deviation of Eu^{3+} ions from the D_{2h} or C_{2h} sites in the SnO_2 nano-crystals [30,33]. In other words, Eu^{3+} ions located at both environments of the nano-crystals and the glassy matrix might be sensitized by the SnO_2 semiconductor. To further verify this, the decay curves of the $^5D_0 \rightarrow {}^7F_1$ emission at 588 nm and the $^5D_0 \rightarrow {}^7F_2$ one at 614 nm in the 0.5 mol% Eu^{3+} doped glass ceramic, under the indirect excitation at 335 nm, were measured as shown in Fig. 6. As a comparison, the decay curve of the $^5D_0 \rightarrow {}^7F_1$ emission at 588 nm in the glass without SnO_2, under 465 nm excitation, is also shown in Fig. 6, which shows a similar decay behavior to that of the 614 emission for the glass ceramic under the indirect excitation. The decay lifetimes were calculated by the equation

$$\tau_{exp} = \int I(t)dt/I_p \quad (1)$$

where $I(t)$ represents the function of the luminescence intensity on the time t, and I_p the peak intensity of the decay curve, as shown in Fig. 6. The lifetime of 1.9 ms for the 614 nm emission under the indirect excitation is near that of 2.0 ms for the emission of the glass, which confirms that the former emission is ascribed to the Eu^{3+} ions located in the glass matrix. The long lifetime of 8.4 ms validates the 588 nm emission under the indirect excitation originated mainly from the Eu^{3+} ions at the C_{2h} or D_{2h} sites in SnO_2. According to the Förster theory, the energy transfer is a very short-range effect, and the energy transfer efficiency is dramatically reduced when the distances between the energy donors and acceptors go beyond the Förster range [34,35]. Obviously, only the Eu^{3+} ions located near the nano-crystals could benefit from the energy transfer and thus contribute to the broad band emission centered at 614 nm under the indirect excitation. Based on the results and discussions stated above, the energy transfer behavior between the SnO_2 nano-crystals and the Eu^{3+} ions in the glass ceramic is shown in Fig. 7.

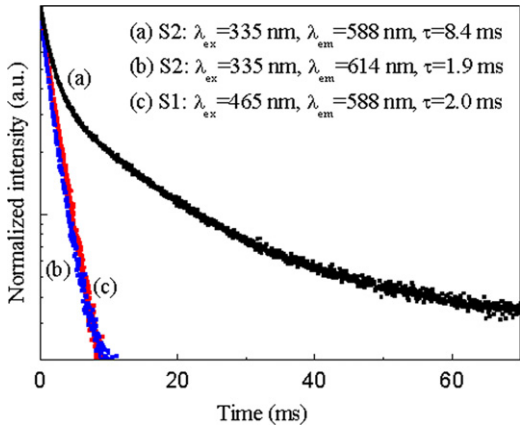

Fig. 6. PL decay curves of 0.5 mol% Eu^{3+} doped glass ceramic under 335 nm excitation: (a) monitored at 588 nm; (b) monitored at 614 nm and (c) PL decay curve of 0.5 mol% Eu^{3+} doped glass without SnO_2 under 465 nm excitation monitored at 588 nm. (S1: glass without SnO_2; S2: glass ceramic).

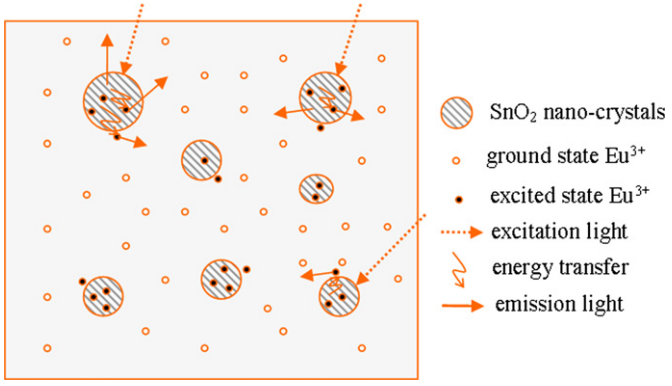

Fig. 7. Schematic diagram showing energy transfer behavior in Eu^{3+} doped glass ceramic embedding SnO_2 nano-crystals.

4. Conclusions

Eu^{3+} doped transparent glass ceramics with SnO_2 nano-crystals homogenously embedding in the oxide glassy matrix were successful prepared. The semiconductor nano-crystals displayed a broad blue emission band. Sensitized by the SnO_2 nano-crystals, the Eu^{3+} ions yielded intense visible emission under ultraviolet excitation. Some of the Eu^{3+} ions were found incorporated in the SnO_2 lattices by substituting Sn^{4+} ions at the C_{2h} or D_{2h} sites, and exhibited much longer luminescent decay lifetime than those residing in the glassy matrix. It was experimentally evidenced that the energy transfer from SnO_2 to Eu^{3+} is closely related to the distribution of Eu^{3+} ions.

Acknowledgments

This work was supported by Science and Technology Projects of Fujian (2009HZ0006-1) and National Natural Science Foundation of China (10974201, 50902130).

References

[1] J. Planelles-Aragó, B. Julián-López, E. Cordoncillo, P. Escribano, F. Pellé, B. Viana, C. Sanchez, J. Mater. Chem. 18 (2008) 5193–5199.
[2] W. Luo, R. Li, X. Chen, J. Phys. Chem. C 113 (2009) 8772–8777.
[3] W. Chen, J.O. Bovin, A.G. Joly, S. Wang, F. Su, G. Li, J. Phys. Chem. B 108 (2004) 11927–11934.
[4] W. Luo, R. Li, G. Liu, M.R. Antonio, X. Chen, J. Phys. Chem. C 112 (2008) 10370–10377.
[5] S. Sapra, A. Prakash, A. Ghangrekar, N. Periasamy, D. Sarma, J. Phys. Chem. B 109 (2005) 1663–1668.
[6] S. Monticone, R. Tufeu, A.V. Kanaev, J. Phys. Chem. B 102 (1998) 2854–2862.
[7] L. Spanhel, M.A. Anderson, J. Am. Chem. Soc. 113 (1991) 2826–2833.
[8] H. Masai, T. Toda, T. Ueno, Y. Takahashi, T. Fujiwara, Appl. Phys. Lett. 94 (2009) 151908.
[9] J.H. Shin, G.N.V. Hoven, A. Polman, Appl. Phys. Lett. 66 (1995) 2379–2382.
[10] M. Fujii, M. Yoshida, Y. Kanzawa, S. Hayashi, K. Yamamoto, Appl. Phys. Lett. 71 (1997) 1198.
[11] V.Y. Timoshenko, M.G. Lisachenko, O.A. Shalygina, B.V. Kamenev, D.M. Zhigunov, S.A. Teterukov, P.K. Kashkarov, J. Appl. Phys. 96 (2004) 2254–2260.
[12] F. Priolo, G. Franzò, S. Coffa, A. Carnera, Phys. Rev. B 57 (1998) 4443–4455.
[13] N.Q. Vinh, S. Minissale, B.A. Andreev, T. Gregorhkevica, J. Phys. Condens. Matter 17 (2005) S2191–S2195.
[14] N.O. Dantas, E.O. Serqueira, A.P. Carmo, M.J.V. Bell, V. Anjos, G.E. Marques, Opt. Lett. 35 (2010) 1329–1331.
[15] J. Bang, H. Yang, P. Holloway, J. Chem. Phys. 123 (2005) 084709.
[16] A.C. Yanes, J.D. Castilli, M.T. Torres, J. Peraza, Appl. Phys. Lett. 85 (2004) 2343–2345.
[17] N. Wan, J. Xu, T. Lin, X. Zhang, L. Xu, Appl. Phys. Lett. 92 (2008) 201109.
[18] B. Julián, J. Planelles, E. Cordoncilli, P. Escribano, P. Aschehoug, C. Sanchez, B. Viana, F. Pellé, J. Mater. Chem. 16 (2006) 4612–4618.
[19] T. Hayakawa, S.T. Selvan, M. Nogami, J. Sol–Gel Sci. Technol. 19 (2000) 779–783.
[20] M. Fukushima, N. Managaki, M. Fujii, H. Yanagi, S. Hayashi, J. Appl. Phys. 98 (2005) 024316.

[21] Y. Yu, D. Chen, Y. Wang, P. Huang, F. Weng, M. Niu, Phys. Chem. Chem. Phys. 11 (2009) 8774–8778.
[22] Y. Wang, X. Jiang, Y. Xia, J. Am. Chem. Soc. 125 (2003) 16176–16177.
[23] B. Cheng, J.M. Russell, W. Shi, L. Zhang, E.T. Samulski, J. Am. Chem. Soc. 126 (2004) 5972–5973.
[24] J.R. Heath, Science 270 (1995) 1315–1316.
[25] M. Nogami, T. Enomoto, T. Hayakawa, J. Lumin. 97 (2002) 147–152.
[26] T. Moon, S.T. Hwang, D.R. Jung, D. Son, C. Kim, J. Kim, M. Kang, B. Park, J. Phys. Chem. C 111 (2007) 4164–4167.
[27] A. Kar, A. Patra, J. Phys. Chem. C 113 (2009) 4375.
[28] F. Gu, S. Wang, M. Lü, G. Zhou, D. Xu, D. Yuan, J. Phys. Chem. B 108 (2004) 8119–8123.
[29] H. Chen, S. Xiong, X. Wu, J. Zhu, J. Shen, Nano Lett. 9 (2009) 1926–1931.
[30] J. Chen, J. Wang, F. Zhang, D. Yan, G. Zhang, R. Zhuo, P. Yan, J. Phys. D—Appl. Phys. 41 (2008) 105306.
[31] W. Fan, S. Song, J. Feng, Y. Lei, G. Zheng, H. Zhang, J. Phys. Chem. C 112 (2008) 19939–19944.
[32] E.A. Morais, S.J.L. Ribeiro, L.V.A. Scalvi, C.V. Santilli, L.O. Ruggiero, S.H. Pulcinelli, Y. Messaddeq, J. Alloys Compd. 344 (2002) 217–220.
[33] H.P. You, M. Nogami, J. Appl. Phys. 95 (2004) 2781–2785.
[34] M. Lessard-Viger, M. Rioux, L. Rainville, D. Boudreau, Nano Lett. 9 (2009) 3066–3071.
[35] S. Brovelli, N. Chiodini, F. Meinardi, A. Monguzzi, A. Lauria, R. Lorenzi, B. Vodopivec, M.C. Mozzati, A. Paleari, Phys. Rev. B 79 (2009) 153108.